RESEARCH ARTICLE | NOVEMBER 21 2014

Photo-crystallization in a-Se layer structures: Effects of film-substrate interface-rigidity

G. P. Lindberg; T. O'Loughlin; N. Gross; ... et. al

Journal of Applied Physics 116, 193511 (2014)
https://doi.org/10.1063/1.4902166

Photo-crystallization in a-Se layer structures: Effects of film-substrate interface-rigidity

G. P. Lindberg,[1] T. O'Loughlin,[2] N. Gross,[1] A. Mishchenko,[3] A. Reznik,[3] S. Abbaszadeh,[4] K. S. Karim,[4] G. Belev,[5] and B. A. Weinstein[1]
[1]*SUNY at Buffalo, Department of Physics, Buffalo, New York 14260-1500, USA*
[2]*SUNY at Buffalo, Department of Chemistry, Buffalo, New York 14260, USA*
[3]*Lakehead University, 955 Oliver Road, Thunder Bay, Ontario P7B 5E1, Canada*
[4]*University of Waterloo, Waterloo, Ontario N2L 3G1, Canada*
[5]*University of Saskatchewan, Saskatoon, Saskatchewan S7N 5A9, Canada*

(Received 26 June 2014; accepted 9 November 2014; published online 21 November 2014)

Amorphous selenium (a-Se) films deposited on rigid substrates can undergo photo-induced crystallization (PC) even at temperatures (T) well below the glass transition, $T_g \sim 313$ K. Substrate-generated shear strain is known to promote the PC process. In the present work, we explore the influence of different substrates (Si and glass), and different film-layer-substrate combinations, on the PC in a variety of a-Se films and film-structures. The intermediate layers (indium tin oxide and polyimide) are chosen to promote conductivity and/or to be a buffer against interface strain in structures of interest for digital imaging applications. The PC characteristics in these samples are evaluated and compared using optical microscopy, atomic-force microscopy, Raman mapping, and T-dependent Raman spectroscopy. Both the presence of a soft intermediate layer, and the thermal softening that occurs for T increasing through T_g, inhibit the tendency for the onset of PC. The extensive PC mapping results in the wide range of samples studied here, as well as the suppression of PC near T_g in this array of samples, strongly support the *generality* of this behavior. As a consequence, one may expect that the stability of a-Se films against PC can be enhanced by decreasing the rigidity of the film-substrate interface. In this regard, advanced film structures that employ flexible substrates, soft intermediate layers, and/or are designed to be operated near T_g should be explored. © *2014 AIP Publishing LLC*. [http://dx.doi.org/10.1063/1.4902166]

I. INTRODUCTION

Stabilization of amorphous selenium (a-Se) films against photo-crystallization (PC) in advanced multi-layer imaging devices based on the photoactive properties of a-Se is important for the success of many applications.[1–3] However, a full understanding of the factors that control PC in a-Se films and film structures for different substrates, growth geometries, and operating temperatures remains elusive in spite of studies by many researchers.[4] Early experiments[5–10] primarily used optical and electron microscopy to study the growth and morphology of crystalline domains, which form in the stable trigonal Se (t-Se) phase. It was established that crystallization initiates preferentially at the substrate interface[6–8] that strain is an important factor in this tendency,[9,10] and that crystallization is enhanced by light.[7–10] Subsequent studies have employed Raman spectroscopy,[11–14] x-ray diffraction, and atomic force microscopy[15,16] to explore aspects of the PC process related to the microscopic changes in structure that drive the *primary* nucleation of t-Se domains. There is a broad consensus that these changes are mediated at the atomic level by a variety of bonding defects, such as dangling bonds and valence alternation pairs.[17]

Here, we employ co-localized Raman mapping and atomic-force microscopy (AFM), Raman spectroscopy, and optical microscopy to probe the *secondary* growth (to μm size) of t-Se domains in a-Se films deposited on glass and Si substrates with or without intermediate coatings of indium-tin oxide (ITO) and/or polyimide. Specifically, we explore the spatial profile of *PC-spots* (crystallized spots created by laser exposure), and the temperature dependence of the PC onset time, in these samples, whose structures are of interest for potential avalanche,[1] metal-semiconductor,[18,19] and CCD[20] applications. In prior work on the PC of a-Se in HARP[1] (High-gain Avalanche Rushing Photoconductor) devices, Tallman *et al.*[14] reported a surprising discontinuous *increase* in the PC onset time as a function of *increasing temperature* near the glass transition $T_g \sim 313$ K. Preliminary results on other glass-deposited a-Se structures found similar jumps in the PC onset times near T_g, but the sizes varied widely.[21] Reference 21 also gives a brief account of early Raman and AFM mapping studies on a 2-year old a-Se/ITO/glass sample that was resistant to PC, and it was suggested that reduced shear strain at the film-substrate interface in this aged film was the cause of its resistance to PC.

The current investigation tests the generality of our earlier results by reporting experiments on a wider range of a-Se films, and clarifies more completely the explanation of the connection between the strain and thermal aspects of the observed effects. Measurements on new a-Se films grown on Si substrates or in different laboratories are presented and compared to the earlier work, much more extensive mapping studies on the new and earlier samples are presented, and the polymerization model[10] used to account for the related strain and thermal effects is discussed in greater detail. This work

adds strong support to the idea that reduction of substrate-generated interface strain can be applied to moderate the tendency for PC in a-Se films. An example of stabilization against PC by depositing a soft polymer layer between an a-Se film and its substrate is seen to have encouraging results in a device-like structure.

II. EXPERIMENT

The samples studied are vapor-grown a-Se films (16–22 μm thick) deposited either directly on glass or on silicon substrates, or deposited on the following layer(s)/glass structures: ITO/glass, polyimide/glass, and polyimide/ITO/glass. The thickness of the intermediate ITO and polyimide layers are 160 nm and 1 μm, respectively.[18] The a-Se films contain $\leq$0.2% As. They were freshly deposited, except for an a-Se/ITO/glass film that was shelf-stored for two years in ambient light. Polyimide is found to be a useful blocking contact between ITO and the photoactive a-Se film.[18]

Co-localized Raman–AFM maps are recorded with a Horiba J-Y LabRam model HR800 spectrometer linked to an AIST-NT SmartSPM 1000 AFM unit. PC is induced using 632 nm laser light at a power of 1 mW focused (n.a. = 0.7 lens) through the film at the film-substrate interface. The flux at the focus is $\sim$0.15 μW/μm^2 (decreased from 0.5 μW/μm^2 at the surface, including absorption and refractive index corrections). We estimate a laser heating above room temperature of $\Delta T \sim 30$–40 C from the observed shift in the Raman spectrum.[22] The Raman mapping is performed using 632 nm or 671 nm laser lines at 10^{-2} lower power focused at the film-air surface to allow comparison with the AFM surface profiles. The Raman maps are recorded with a 0.5 μm step size ($\sim$1/3 the focused beam waist), and the resolution of the AFM profiles is 25 nm. The sharp focus of the Raman mapping system and the film absorption reduces the flux by $\sim 10^{-4}$ at the film-substrate interface where PC initiates. Consequently, significant additional PC does not accumulate during the 10 s dwell time at each spatial position.

A different apparatus is used to study the onset-time of PC as a function of temperature. In this case, we employed conventional Raman spectroscopy recorded with the 647 nm line of a Kr^+-laser at a flux of 1.3 μW/μm^2. The same laser beam is used to induce and probe the PC, and exposure is continuous until the PC onset is observed (durations of $\sim$5–500 min.) The measurement system is described elsewhere.[14] The local temperature, estimated from the ratio of the Stokes to anti-Stokes Raman signals, is varied between 285 K–345 K (uncertain to $\pm$5 K.) The local temperatures are used in the discussion of the onset-time results. The recorded Raman spectra monitor the frequency region 200 cm^{-1}–300 cm^{-1}, containing the strong A1-symmetry peaks of t-Se (237 cm^{-1}) and a-Se (256 cm^{-1}).[23,24] PC is detected by an increase in strength (from zero intensity) of the t-Se peak and a simultaneous decrease of the a-Se peak. See Ref. 14 for further details.

III. SPATIAL MAPPING OF PC PROFILES

Figure 1 shows optical micrographs, taken in transmission and reflection, of PC-spots produced in two different samples, both having the film structure a-Se/ITO/glass. In Fig. 1(a), the microscope is focused on the sample's top surface (i.e., the a-Se-air surface). The left-hand (LH) and right-hand (RH) spots are created by exposing the film to focused laser light directly through the glass substrate and through the film's top surface, respectively. Both exposures give the same spot morphology, an oval shape on the top surface, and "wing" like lateral shadows that extend up from the a-Se film's bottom surface (i.e., the a-Se/ITO interface). This morphology is confirmed by the reflection micrographs in Figs. 1(b) and 1(c), recorded, respectively, for the RH spot in Fig. 1(a) and for a PC-spot produced in another a-Se/ITO/glass sample.

Additional examination of the latter spot under transmitted light at low and high magnifications (Figs. 1(d) and 1(e)) reveals the individual t-Se domains. Previous work has shown that these domains are generally in the shape of pyramidal cylindrites,[5–10] with the apex growing toward the top surface of the a-Se film and the base at the films bottom surface (i.e., here, the a-Se/ITO interface.) The driving

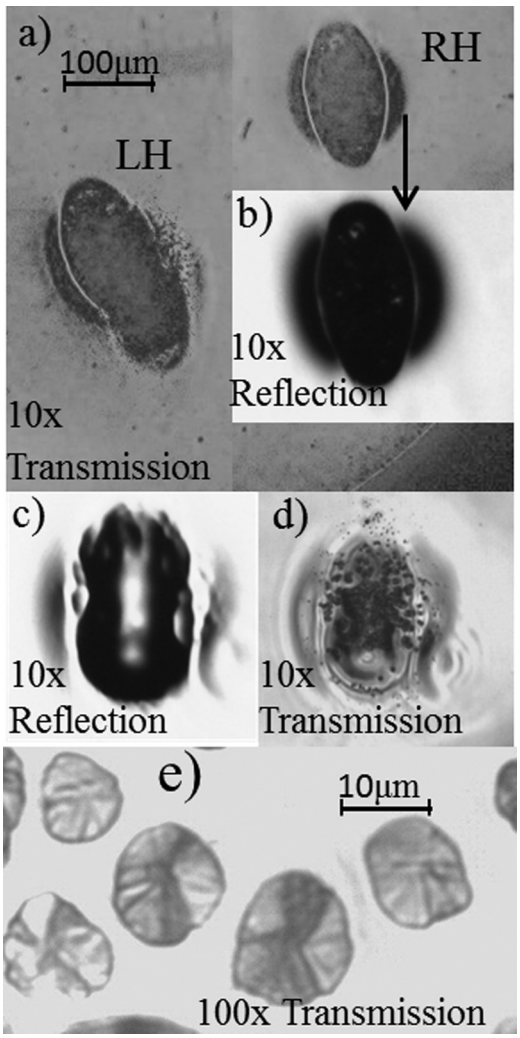

FIG. 1. Microphotographs of PC-spots in two a-Se/ITO/Glass samples: (a) spots created by laser-light incident on the glass (LH) and film (RH) sides; (b) reflection image of RH spot; (c) and (d) analogous images of a PC-spot in another a-Se/ITO/Glass sample; and (e) high-power view of t-Se cylindrites in latter spot.

mechanism for this geometry is thought to be substrate-induced strain transmitted to the Se layer, which causes the lateral growth of t-Se near the substrate to be faster than the growth normal to the substrate. The shapes of the crystallites in Fig. 1(e) are consistent with this habit of growth.

In Figure 2, we show a Raman mapping profile of a PC-spot in a film of a-Se deposited on a device-grade silicon substrate. This profile charts the intensities of the a-Se and t-Se A1 Raman modes as a function of the surface position of the probing laser. A typical scan across the center of the spot, showing the fractional contributions of each peak to the total intensity, is illustrated in the RH inset. The central region is strongly dominated by the t-Se A1 peak (at 237 cm^{-1}), whereas around the spot, the a-Se A1 peak (at 256 cm^{-1}) becomes dominant. The boundary region of mixed a-Se and t-Se is $\sim 2\,\mu m$ wide (LH inset). The Raman intensities indicate that the central volume under the laser spot contains $\gtrsim$90% t-Se. A co-localized AFM map of the same PC-spot (Figure 3) reveals the areal and depth topologies in greater detail. Figs. 3(a) and 3(b) show three dimensional views of the spot from two different angles. Fig. 3(c) is a cut away showing the height difference across the center of the spot. There are two depressions surrounding the oval shaped raised center. Comparing to the Raman map in Fig. 2, we establish that the raised region consists mainly of t-Se ($\gtrsim$ 90% within the dashed circles), and the fraction of a-Se in the depressions increases rapidly as one moves outward. The total change in height is $\sim 3\,\mu m$. The PC results in this a-Se/Si sample suggest that a focused laser beam incident through the film tends to draw the growth of t-Se domains toward the film surface. Shear stress due to laser-tweezing, and local heating, are two factors that may promote this behavior in the presence of a tightly focused pump beam. Similar behavior was noted for other samples in Ref. 21. The depth profile most likely reflects the reaction of the film to the 12% density increase in the central t-Se component compared to the density of the surrounding a-Se. As PC initiates and crystallites grow and agglomerate to saturation under the focused laser beam, this

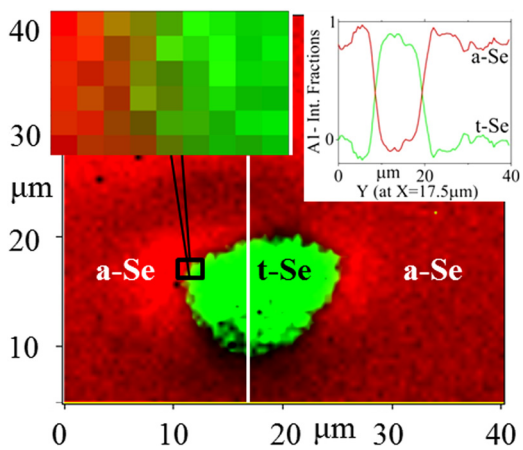

FIG. 2. Raman map of PC-spot in an a-Se film on Si, profiling the intensities of the t-Se (green online) and a-Se (red online) A1 Raman peaks. RH inset shows a y-axis scan at $x = 17.5\,\mu m$ (white line) giving the fraction of the total intensity contributed by each peak. LH inset is a blow-up of a-Se/t-Se boundary. Probing laser was focused at the film-air interface.

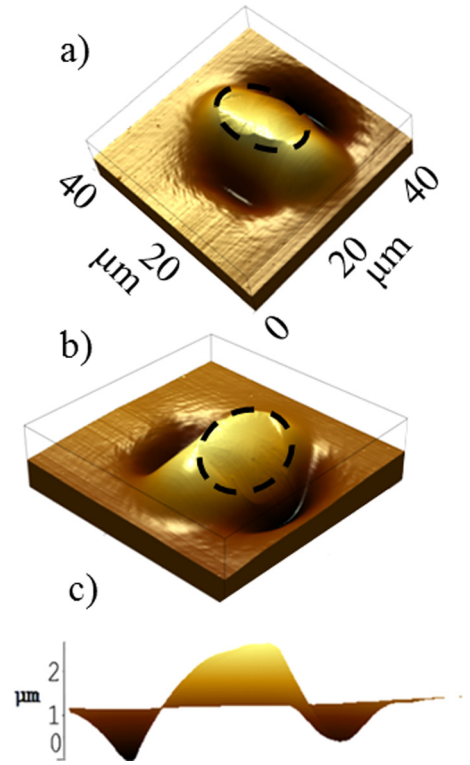

FIG. 3. AFM maps of same PC-spot shown in Fig. 2. (a) and (b) 3d-views from two angles; dashed black circles outline t-Se high-content region in Fig. 2. (c) Depth profile across spot center.

density increase causes an anisotropic growth-induced material flow that acts to pull Se in from the surrounding matrix. The radial asymmetry in the spot is probably due to light polarization effects.[12,25] Figure 4 is a schematic representation of the change in film morphology observed in the Raman and AFM maps of Figs. 2 and 3.

Figure 5 documents an attempt to create PC in an early a-Se/ITO/glass film that was shelf-aged for two years under room light conditions. This film showed signs of appreciable changes including flaking, areas that had crystalized, as well as regions that were still amorphous, as confirmed by low-power Raman mapping. We found it difficult to induce PC in the a-Se regions of this sample without also producing physical damage, in contrast to our results on the other samples (which were not older than 4 months.) The AFM profile in Fig. 5(a) shows a raised spot created by a $0.5\,\mu W/\mu m^2$ flux of 671 nm light. A Raman map of the $10\,\mu m^2$ area centered on the swelling detects only a-Se in the entire square (Fig. 5(b) map and insert). Subsequently, another AFM scan of this square (Fig. 5(c)) reveals that wherever the probing laser

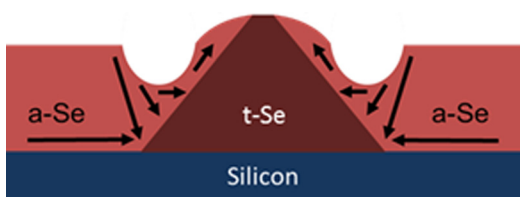

FIG. 4. Model of change in morphology under the focused laser spot for saturated growth of PC in an a-Se film on a rigid Si substrate. A boundary trough forms due to the density increase in t-Se.

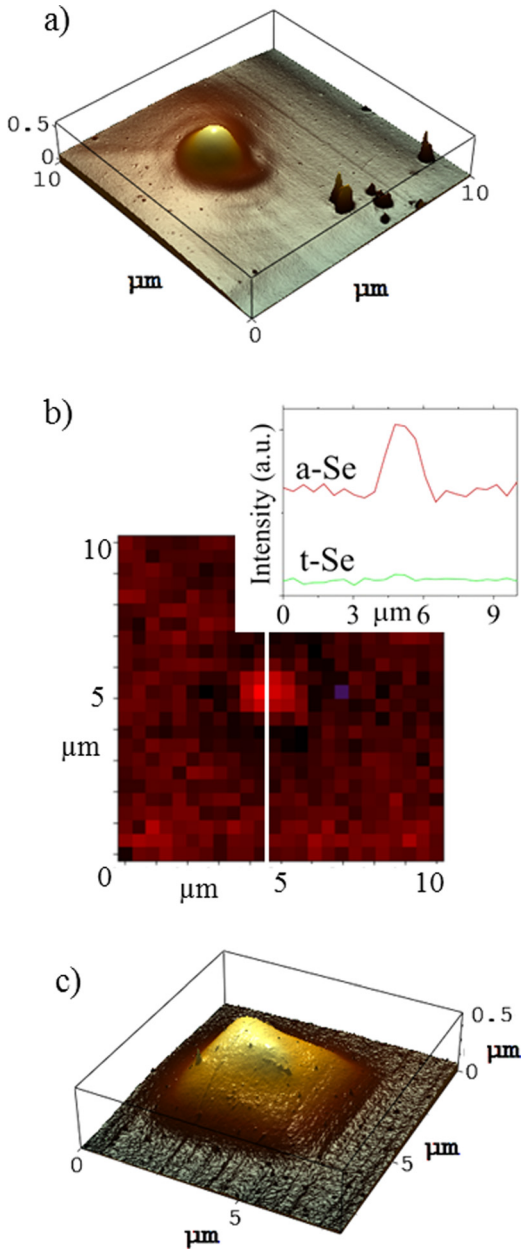

FIG. 5. Results of attempt to produce PC in an aged a-Se/ITO/Glass sample. (a) 3d-AFM profile of a laser-induced spot; (b) Raman map of 10 μm^2 area around spot. Only a-Se (red online) is found. Inset is y-axis scan at x = 4.2 μm of a-Se and t-Se A1 intensities; (c) 3d-AFM map of subsequent swelling in a-Se phase caused by Raman probe.

has been incident, the a-Se film becomes raised by ~0.5 μm without being crystallized and without forming sunken regions. The most likely explanation is that the film-substrate adhesion has degraded in this film during its two year storage. This might happen through changes in the a-Se network that favor photo-expansion instead of PC, as is sometimes found.[26–28] If the film-substrate adhesion degrades, the substrate strain which tends to promote PC is weakened, consistent with the observed difficulty in crystallizing this film.

Besides the aged a-Se/ITO/glass film just discussed, we find that freshly grown structures containing a polyimide layer between the a-Se and the substrate exhibit greatly enhanced stability against PC. In fact, our Raman spectroscopy results on the a-Se/polyimide/glass and the a-Se/polyimide/ITO/glass samples observe *no onset of PC whatsoever* in the temperature range investigated, 280 K–345 K. Weak adhesion is again a possibility. However, we discount this since these samples exhibited good electronic response in feasibility tests for photo-sensor applications.[18,29] Rather, we attribute the observed stabilization against PC to the mechanical softness of the polyimide layer, which is able to insulate the a-Se from the effects of substrate strain.

IV. TEMPERATURE DEPENDENCE OF PC ONSET

The onset-time of PC in the a-Se films is determined by monitoring changes in the Raman spectrum. The following analysis is used to improve the accuracy over earlier studies.[14,21] A reference Raman line-shape is established for a given location on the film by fitting the Raman spectrum recorded on initial ($\leq$5 min) laser exposure at that spot. We assume this line-shape reflects the zero-time state of the film, and has no (or minimal) t-Se component. This reference is subtracted from each subsequent spectrum after scaling to match the observed height of the a-Se A1 peak. As the PC progresses, this difference of spectra gives a peak at 237 cm^{-1}, whose intensity reflects the amount of t-Se that is present under the laser spot. The onset of PC is taken as the minimum laser-exposure time for this intensity to exceed twice the RMS noise in the measured spectra.

Figure 6 compares the observed onset time for PC as a function of temperature in three films. The error bars reflect the uncertainty that would result from a ±25% variation of the RMS spectral noise. In Figs. 6(a) and 6(b), the film structures are 16 μm a-Se on ITO/glass, and, in Fig. 6(c), the structure is 16 μm a-Se on uncoated glass. The onset times for the latter film do not exceed 30 min, short compared to those found for the films grown on ITO/glass (up to 400 min). This indicates that films deposited on plain glass substrates may be more prone to PC than those deposited on ITO-coated glass substrates.

The results in Fig. 6 reveal that a discontinuous increase in the PC onset-time occurs with increasing temperature near the a-Se glass transition ($T_g \sim 313$ K). At other temperatures, the expected behavior is seen—shorter onset-times at higher temperatures. The discontinuities, which are ~300 min in Fig. 6(a) and ~15 min in Figs. 6(b) and 6(c), exceed the uncertainty in each case, although the Fig. 6(c) result may perhaps be judged borderline. This variation of the jump in PC onset-time near T_g for different glass-deposited a-Se film structures is consistent with the preliminary results in Ref. 21. In addition, in our work[14] on Se layers in HARP targets, a stronger discontinuity is found that leads to a "dead zone" at temperatures of 303 K–318 K, in which no PC could be produced during time periods extending up to 18 h.

The discontinuities in the PC onset-time as a function of temperature strongly indicate that the PC growth kinetics is mediated by competing mechanisms near to the a-Se glass transition. This was suggested in Ref. 14 to explain the HARP target results, and the present findings provide further confirmation for a more diverse range of a-Se film samples. The

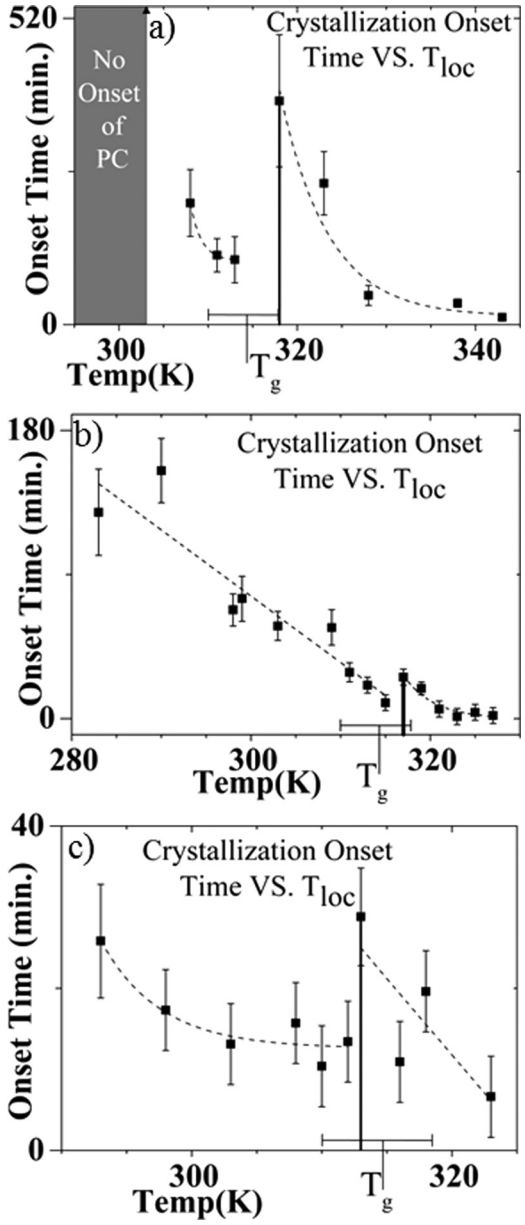

FIG. 6. Comparison of the effect of temperature on the Raman-observed PC onset times in (a) an a-Se/ITO/Glass sample, (b) a similar sample fabricated in a different laboratory, and (c) an a-Se/Glass sample. Note jump in the onset time on heating through T_g in each sample. Data in (a) and (c) are taken from prior experiments[21] after revised analysis by the more accurate method described in the text.

competing mechanisms can be understood in terms of a model proposed by Stephens,[10] which will be discussed further in Sec. V. We point out that some of the observed differences in the PC behavior of our a-Se films may be due to their preparation in different laboratories with different surface cleaning procedures prior to a-Se deposition. However, our results for both the mapping and onset-time experiments provide convincing evidence that the rigidity of the interface between an a-Se film and its substrate can mediate the onset of PC.

V. DISCUSSION

Our experiments on PC in a-Se films reveal a number of interesting substrate-related effects that operate by complex mechanisms. However, the underlying physics is straightforward, and it is instructive to present a brief summary.

At the atomic scale, PC in a-Se proceeds by bonding-defect reactions, in which the chain fragments and rings of the a-Se matrix linkup to form the ordered t-Se structure[4,17]—triad spiral c-axis-chains set on a hexagonal basal array.[4,17] The defect configurations of the Se lone-pair electrons are generally thought to mediate these reactions. The bond changes enable the nucleation of t-Se embryos large enough (~few nm) to sustain further growth,[9] and also act at the t-Se/a-Se interface to drive the secondary growth to μm-size t-Se domains.

The Stephens model[10] addresses the secondary growth process. It treats a-Se as a disordered array of polymer chain segments and 8-fold rings (~4%),[30] in which the mean number $\bar{P}$ of Se_8 units in the chain segments depends on temperature and internal stress. A thermodynamic approach[31] is used that does not require knowledge of the specific defect reactions. The internal stress arises from the 12% density increase in t-Se relative to a-Se. The stress is tensile in the a-Se matrix around a t-Se domain, and, for good adhesion, the stress is enhanced near a rigid substrate by the latter's stiffness. Additional chain segments link to the t-Se domains by processes that involve viscous flow or chain-end rotation, and a smaller $\bar{P}$ increases the probability for segments to find geometries that favor t-Se. The kinetic energy needed to drive these bonding changes can be supplied by temperature and/or photons. The tensile stress around a t-Se domain acts to decrease $\bar{P}$ in the nearby a-Se matrix, and so provides another driving potential for t-Se growth according to[10]

$$\bar{P} \sim \left[\frac{M_o K' - 1}{K}\right]^{1/2} \exp\left(\frac{-\sigma_e \Delta V}{2kT}\right). \quad (1)$$

The effective hydrostatic portion of the stress is σ_e, ΔV is the local volume increase on creating two chain ends, K and K′ are T-dependent rate constants, and M_o is the density of Se_8 units. Similar thermodynamic considerations could be applied to calculate $\bar{P}$ for more recent structural models, in which, e.g., a-Se is viewed as a collection of chain fragments with a balance of t-Se-like and ring-Se-like second nearest neighbor configurations.[32] The Raman detection limit is such that the onset time observed here should correspond to ~1%–2% t-Se in the film-volume under the laser beam. For temperatures $T < T_g$, the film is rigid and can support σ_e. At the t-Se/a-Se boundary of a domain that lies near the substrate, $\bar{P}$ is decreased by σ_e, thereby promoting t-Se growth. As T is raised, thermal energy drives the growth faster. We observe shorter onset times, providing the a-Se matrix continues to support σ_e. This drastically changes at the glass transition with softening of the a-Se matrix. The resulting decrease in σ_e *competes* with increasing T in the overall effect on $\bar{P}$. One expects a sudden increase in the onset time as T is raised from below to above T_g, in agreement with our findings. At still higher temperatures, the effect of σ_e vanishes. Crystallization becomes primarily a thermally driven process that is only assisted by light. The onset time for crystallization should again fall, as is observed.

Our results for the two a-Se film structures that contain a soft intermediate layer of polyimide, and for the film with degraded adhesion, support the validity of this model, since the rigidity of the film-substrate interface is greatly reduced in these samples. In particular, the former samples show that it is possible to exploit the use of intermediate polymer layers to control the transmission of strain from a substrate into an a-Se film device. There are many applications where this is desirable. Here, it is employed to stabilize the a-Se against PC, while preserving the electrical contact characteristics needed for a device to operate as a sensitive photodetector.[18]

VI. SUMMARY

Raman scattering, AFM, and optical microscopy are used to investigate PC in a-Se film structures deposited on glass and Si substrates with or without intermediate ITO and/or polyimide coatings, geometries of technological interest. We study the occurrence, growth morphology, and onset time of the PC in a-Se for the different film-substrate interfaces, and for temperatures that span the glass transition. Our AFM profiles show a distinct trough around PC-spots, reflecting the action of tensile strain arising from the 12% densification in t-Se regions. The temperature dependence of the PC onset time near T_g (± 3 K) exhibits a jump discontinuity in which a small rise in temperature causes a slower onset of PC. Thus, there is a temperature regime in which supplying more thermal energy has the counter-intuitive effect of enhancing stability against PC. Our results demonstrate the generality of this effect for films subject to strain from a rigid film-substrate interface. In contrast, we find that *no PC occurs* in three samples where either weak adhesion, or a soft polyimide intermediate layer, relieves this interface-strain. Our results are in accord with the theory of Ref. 10 for PC in a-Se films, a polymerization model that has been successful in explaining the ability of tensile strain to promote PC. Competition between the effects of strain and temperature as the a-Se softens on heating above T_g causes the discontinuity in the PC onset time. The problematic occurrence of PC in a-Se film devices might be avoided by engineering structures without a rigid film-substrate interface—as is found here by introducing a soft polyimide layer into the interface region. Further investigations along these lines should be undertaken.

ACKNOWLEDGMENTS

Partial support of the work at SUNY Buffalo by NSF Grant No. CHE1126301, and by a grant from the Thunder Bay Regional Research Institute, Ontario, C.A. is gratefully acknowledged. Thanks are also due to the Natural Sciences and Engineering Research Council of Canada, the Ontario Research Fund—Research Excellence Program, and the Canadian Institutes of Health Research for their finiancial support. We are indebted to S. O. Kasap and D. M. Hunter for assistance in providing samples and fruitful discussions.

[1]M. Kubota, T. Kato, S. Suzuki, H. Maruyama, K. Shidara, K. Tanioka, K. Sameshima, T. Makishima, K. Tsuji, T. Hirai, and T. Yoshida, IEEE Trans. Broadcast. **42**(3), 251–258 (1996).
[2]J. A. Rowlands, D. M. Hunter, and N. Araj, Med. Phys. **18**(3), 421–431 (1991).
[3]S. O. Kasap and J. A. Rowlands, Proc. IEEE **90**(4), 591–604 (2002).
[4]K. Tanaka and K. Shimakawa, *Amorphous Chalcogenide Semiconductors and Related Materials* (Springer, 2011).
[5]J. Dresner and G. B. Stringfellow, J. Phys. Chem. Solids **29**(2), 303–311 (1968).
[6]K. S. Kim and D. Turnbull, J. Appl. Phys. **44**(12), 5237–5244 (1973).
[7]K. S. Kim and D. Turnbull, J. Appl. Phys. **45**(8), 3447–3452 (1974).
[8]R. Clement, J. C. Carballes, and B. de Cremoux, J. Non-Cryst. Solids **15**(3), 505–516 (1974).
[9]G. Gross, R. B. Stephens, and D. Turnbull, J. Appl. Phys. **48**(3), 1139–1148 (1977).
[10]R. B. Stephens, J. Appl. Phys. **51**(12), 6197 (1980).
[11]A. A. Baganich, V. I. Mikla, D. G. Semak, A. P. Sokolov, and A. P. Shebanin, Phys. Status Solidi B **166**(1), 297–302 (1991).
[12]V. V. Poborchii, A. V. Kolobov, and K. Tanaka, Appl. Phys. Lett. **72**(10), 1167 (1998).
[13]A. Roy, A. V. Kolobov, and K. Tanaka, J. Appl. Phys. **83**(9), 4951–4956 (1998).
[14]R. E. Tallman, B. A. Weinstein, A. Reznik, M. Kubota, K. Tanioka, and J. A. Rowlands, J. Non-Cryst. Solids **354**(40–41), 4577–4581 (2008).
[15]V. K. Tikhomirov, P. Hertogen, G. J. Adriaenssens, C. Glorieux, and R. Ottenburgs, J. Non-Cryst. Solids **227–230**, 732–738 (1998).
[16]T. Innami and S. Adachi, Phys. Rev. B **60**(11), 8284–8289 (1999).
[17]H. Fritzsche, Philos. Mag. B **68**(4), 561–572 (1993).
[18]S. Abbaszadeh, N. Allec, W. Kai, and K. S. Karim, IEEE Electron Device Lett. **32**(9), 1263–1265 (2011).
[19]K. Wang, F. Chen, G. Belev, S. Kasap, and K. S. Karim, Appl. Phys. Lett. **95**(1), 013505 (2009).
[20]D. M. Hunter, G. Belev, S. Kasap, and M. J. Yaffe, Med. Phys. **39**(2), 608–622 (2012).
[21]G. P. Lindberg, T. O'Loughlin, N. Gross, A. Reznik, S. Abbaszadeh, K. S. Karim, G. Belev, D. M. Hunter, and B. A. Weinstein, Can. J. Phys. **92**(7/8), 728–731 (2014).
[22]V. V. Poborchii, A. V. Kolobov, J. Caro, V. V. Zhuravlev, and K. Tanaka, Phys. Rev. Lett. **82**(9), 1955–1958 (1999).
[23]G. Lucovsky, A. Mooradian, W. Taylor, G. B. Wright, and R. C. Keezer, Solid State Commun. **5**(2), 113 (1967).
[24]R. M. Martin, G. Lucovsky, and K. Helliwell, Phys. Rev. B **13**(4), 1383–1395 (1976).
[25]M. L. Trunov, P. M. Lytvyn, S. N. Yannopoulos, I. A. Szabo, and S. Kokenyesi, Appl. Phys. Lett. **99**(5), 051906 (2011).
[26]J. Hegedüs, K. Kohary, D. G. Pettifor, K. Shimakawa, and S. Kugler, Phys. Rev. Lett. **95**(20), 206803 (2005).
[27]R. Lukacs, M. Veres, K. Shimakawa, and S. Kugler, J. Appl. Phys. **107**(7), 073517 (2010).
[28]W. C. Tan, Ph.D. dissertation, University of Saskatchewan, 2006.
[29]S. Abbaszadeh, C. C. Scott, O. Bubon, A. Reznik, and K. S. Karim, Sci. Rep. **3**, 3360 (2013).
[30]P. J. Carroll and J. S. Lannin, Solid State Commun. **40**(1), 81–84 (1981).
[31]A. Eisenberg and A. V. Tobolsky, J. Polym. Sci. **46**(147), 19–28 (1960).
[32]J. C. Mauro and A. K. Varshneya, Phys. Rev. B **71**(21), 214105 (2005).